Insights on estimating urban CO_2 emissions using eddy-covariance flux measurements

Kyung-Eun Min[1*], Junphil Mun[1], Begie Perdigones[1], Soojin Lee[1], Kyung-Hwan Kwak[2]

[1]School of Earth Sciences and Environmental Engineering, Gwangju Institute of Science and Technology (GIST), Gwangju,
61005, Korea
[2]School of Natural Resources and Environmental Science, Kangwon National University, Chuncheon, 24341, Korea

Correspondence to: Kyung-Eun Min (kemin@gist.ac.kr)

Abstract. Living in an era of government allocated carbon dioxide (CO_2) emissions, knowing the accurate amount of human-induced CO_2 becomes very critical. To this end, an in-depth understanding of CO_2 emissions in urban areas where human activities are concentrated will be of practical help. With this motivation, we quantify CO_2 emission strengths of individual urban activities (i.e. vehicle, industry, heat generation, etc.) based on direct observations of vertical CO_2 exchanges at urban-atmosphere interface using Eddy-Covariance (EC) method at Gwangju, Korea (2017.11-2018.08). Day of week difference analysis, together with varying wind sector, grounded from carefully designed measurement set-up, enables us to assess CO_2 emission factors (*EF*s) free from seasonal bias (i.e. heating and urban vegetation); evaluated *EF*s of traffic from day of week difference was 0.017($\pm$0.011) μmol m^{-2} s^{-1} car^{-1} which is more than 10 times larger than that from simple relation (0.0012$\pm$0.0011 μmol m^{-2} s^{-1} car^{-1}) between CO_2 flux and traffic counts. The CO_2 emissions due to the car manufacturing industry within the fetch and heating when air temperatures were lower than 18 °C were quantified as 103.25($\pm$42.18) μmol m^{-2} s^{-1} and 2.41($\pm$1.71) μmol m^{-2} s^{-1} °C^{-1}, respectively. Urban vegetation uptake was estimated as -1.72 kg C m^{-2} yr^{-1} only with *EF*s traffic inferred from day of week difference indicating possible erroneous estimation in simple relation unless it properly reflects representative seasonal changes in a year. Even though our estimations are conservative *EF*s due to limitations in corrections of horizontal seepage and vertical storage, we found that both *EF*s for traffic and heat in latest emission inventory were more than 2.5 times lower than our estimations which indicate the urgency in bottom-up inventory validations.

1 Introduction

As a mitigation strategy to climate change, most countries in the world are living under the motto of reduction in greenhouse gas (GHG) emission based on global consensus on seriousness and urgency in climate change. In order to realize this, many great deals of efforts are being invested not only reducing carbon dioxide (CO_2) emissions from individual to international levels but also re-recognizing CO_2 emissions as an economic concept via trading, taxing and capping, since this molecule comprises up to 65 % of radiative forcing among human-driven emissions (NOAA, 2018). Thus precise and accurate

Atmospheric
Chemistry
and Physics
Discussions

30   knowledge on anthropogenic CO_2 sources and their emission strengths would be beneficial for establishing effective implementation strategies.

As supportive efforts on this aspect, many different methods have been developed to evaluate CO_2 emission rates, especially in urban settings, where strong signatures of human activities in a society are concentrated due to urbanization (Coutts et al., 2007). Roughly, 30 to 40 % of anthropogenic CO_2 are emitted in urban areas (Satterthwaite, 2008).

35   One of the most common methods to compile CO_2 emission inventory is bottom–up estimation. This method estimates CO_2 emission from various source sectors by adding up each element that emits CO_2 with their emission strength weighted by the degree of vitality in activity; in most countries worldwide, CO_2 emissions from the major factories, automobiles and heating are indirectly compiled via this method based on raw material consumption, traffic volumes, vehicle miles travelled, and energy consumption (Gately et al., 2013; Kennedy et al., 2009; Velasco et al., 2009). The bottom-up method has a strength

40   to encompass most of CO_2 emission-related activities, thus, local, regional, national, and global scale inventory constructions are possible.

However, this approach often reports low bias in estimation, likely due to missing/unknown source components and/or inaccuracies and incompleteness in emission factors (EFs) (Kennedy et al., 2010; Leip et al., 2018) as well as uncertainties in the degree of activity estimations such as anthropogenic activity and land cover (Zhang et al., 2014). For example,

45   unreported land use and/or activities can alter the strength of emission drastically than what is reflected in the bottom-up inventory (Velasco and Roth, 2010). In addition, fixed EFs of vehicle have challenges to reveal true emission during real driving conditions with varying traffic situations as the air–fuel ratio changes as described by Lee et al. (2013). Thus, validations of existing bottom-up inventory to assess its legitimacy via independent methods such as inversion-analysis and/or direct CO_2 flux measurements are required (Hirano et al., 2015).

50   There are other indirect means to estimate CO_2 emissions such as usage of household expenditure to examine its relationship with energy use and the associated carbon emissions (Druckman and Jackson, 2009; Isaksen and Narbel, 2017). Nighttime light data has also been proven to have advantages in calculating CO_2 emissions at finer spatial resolutions (Doll et al., 2006; Ghosh et al., 2010; Lu and Liu, 2014; Shi et al., 2016). Both are beneficial approaches for estimating gross scale CO_2 emission. However, they are still limited for activity-specific emission strength estimation, in addition to the uncertainties in

55   activity measures such as expenditure surveys (Kerkhof et al., 2009) and nightlight data due to sensor saturation in urban cores (Zhang et al., 2017).

Direct observation-based estimation methods are also used. Berkeley Environmental Air-quality & CO_2 Network (BEACO2N) is a relatively new approach using dense networks of small observing nodes to measure urban CO_2 mixing ratio and other atmospheric gases (Shusterman et al., 2018; Turner et al., 2016). Recently, Turner et al. (2020) estimates urban

60   CO_2 emission from observation changes before and during the COVID-19 (Coronavirus Disease 2019) mobility regulations with an aid of atmospheric transport model, since the observing nodes only provide information of mixing ratio rather than the flux of CO_2.

Atmospheric
Chemistry
and Physics
Discussions

Eddy Covariance (EC) flux measurement is a promising method to validate carbon emission inventories, since it directly provides observation-based CO_2 exchanges in urban canopy scale. The CO_2 flux measurements based on EC technique have

65 been utilized to elucidate the degree of natural and anthropogenic carbon transfer across the atmosphere and adjacent surface system (Baldocchi et al., 2001; Sabbatini et al., 2018). EC uses covariance of vertical wind speed and targeted scalar concentration to evaluate the degree of exchanges based on high time resolution observations in precision to capture all signatures in full suite of eddy scales which ranges from sub-seconds to hours (Desjardins, 1974; Katul et al., 2001; Liang and Wang, 2020). This technique was originally developed to evaluate the plant productivity over homogeneous plano-

70 surface (Baldocchi et al., 2001 and references therein), however, its application has been expanded from traditional to the non–ideal environment i.e. urban area (Christen et al., 2011; Coutts et al., 2007; Crawford et al., 2011; Grimmond et al., 2002; Lietzke et al., 2015; Moriwaki and Kanda, 2004; Nemitz et al., 2002), and the number of measurements has grown rapidly over the past two decades (Menzer and McFadden, 2017; Björkegren and Grimmond, 2018; Conte et al., 2018; Goret et al., 2019; Stagakis et al., 2019; Rana et al., 2021; Matthews and Schume, 2022).

75 Applications of EC technique in an urban setting have a strength in CO_2 flux monitoring, since it is capable to capture the signature of exchanges in hours to years in time span (Wofsy et al., 1993) with spatial range which varies from few hundred meters to kilometers (Schmid, 1994) and thus easily covers a city scale. For this reason, several attempts have been made to estimate urban CO_2 emission, as summarized in Table 1. The reported urban CO_2 flux in Table 1 largely varies, but it is possibly due to various environmental settings (e.g. population, traffic, vegetation density as well as its maturity, etc.) where

80 the measurements had been conducted. Generally, urban sites are characterized as net source of CO_2, reported with positive sign in flux.

Table 1. Summary of reported urban/suburban CO_2 flux measurements by eddy covariance technique, together with site characteristics such as land use type and mean canopy and measuring heights (z_h and z_m). Emission factors (*EF*s) for heating and traffic are also listed, if
85 available.

City, Country	Land Use Type	$z_m(z_m/z_h)$ [m]	Flux [μmol m^{-2} s^{-1}]	EFs Heating [μmol m^{-2} s^{-1} °C^{-1}]	Car [μmol m^{-2} s^{-1} car^{-1}]	Reference
Arnhem, Netherlands	Urban	23 (2.1)	5.76	1.483[*]	0.075[*]	Kleingeld et al., 2018
Basel, Switzerland	Urban	41 (2.5)	16.4	0.019[*]	0.011[*]	Lietzke et al., 2015
Beijing, China	Urban	47 (2.8)	13.0	0.34[*]		Liu et al., 2012
Cairo, Egypt	Urban	35 (1.6)	6.18			Burri et al., 2009
Chicago, USA	Suburban	27 (4.29)	3.67			Grimmond et al., 2002
Essen, Germany	Urban	26 (1.7)	9.30			Kordowski and Kuttler, 2010

Firenze, Italy	Urban	33 (1.32)	25.8		Matese et al., 2009
Helsinki, Finland	Urban	26 (3.7)	4.78		0.004	Vesala et al., 2008
Heraklion, Greece	Urban	27 (2.4)	6.77		9.66 $\mu mol\ m^{-2}\ s^{-1®}$	Stagakis et al., 2019
Houston, USA	Urban	60 (10.5)	8.00		0.002[*]	Park and Schade, 2016
Lecce, Italy	Urban	14	7.73			Conte et al., 2018
Łódź, Poland	Urban	37 (3.4)	-5 to 15	0.183-3.499[*]		Pawlak et al., 2011
London, UK	Urban	190 (22)	38.0		a: 4.05-6.89 b: 4.09-5.47×10^{-4}[**]	Helfter et al., 2011
London, UK	Urban	49 (2.2)	33.6	1.95[*]	6.7, 5.2 $\mu mol\ m^{-2}\ s^{-1†}$	Ward et al., 2015
London, UK	Urban	46.4 (2.21)	37.04 – 38.56		27.39 $\mu mol\ m^{-2}\ s^{-1®}$	Björkegren and Grimmond, 2018
Melbourne, Australia	Suburban	40 (3.33)	6.12			Coutts et al., 2007
Mexico City, Mexico	Suburban	37 (3.8)	19.5		1.53-3.87[*]	Velasco et al., 2005
Montreal, Canada	Urban	25 (3.16)	10.17			Bergeron and Strachan, 2011
Münster, Germany	Urban	65 (4.33)	12			Schmidt et al., 2008
Osaka, Japan	Urban	127 (11.9)	1.29 -12.9	0.26[*]		Ueyama and Ando, 2016
Tokyo, Japan	Suburban	29 (4)	5.68 Summer 13.0 winter			Moriwaki and Kanda, 2004
Vancouver, Canada	Urban	24.8 (3.82)	17.0	1.45[*]	11.71 $\mu mol\ m^{-2}\ s^{-1¶¶}$	Crawford and Christen, 2015
Vienna, Austria	Urban	144 (5.8 – 9.6)	13.97	0.72[*]	0.0089, 0.0043$^{©}$	Matthews and Schume, 2022
Gwangju, Korea	**Urban**	**88 (7.1)**	**28.26**	**2.45**	**0.017§**	**This study**

*: simple linear regression; ®: rely on road fraction from land cover than number of cars; **: exponential regression expressed as Flux = $ae^{b\text{Cars}}$; †: traffic counts are not considered but weekdays and weekend fluxes, ¶: unit conversion from daily emission; ©: winter and summer weekday; §: traffic counts difference in weekdays and weekend

Atmospheric
Chemistry
and Physics
Discussions

90 Relatively, less attempts are made to infer CO_2 EFs from EC flux measurements compared to its spatiotemporal analysis which limit the usage of EC flux measurements. Table 1 also lists few studies which evaluated EFs for heating ($EFs_{heating}$) and traffic ($EFs_{traffic}$) from their CO_2 EC flux measurements. $EFs_{heating}$ were inferred from the relationship between observed CO_2 fluxes and temperatures over the heating degree days (HDD, Crawford and Christen, 2015; Kleingeld et al., 2018; Lietzke et al., 2015), while $EFs_{traffic}$ were mostly evaluated from simple linear relation (here after SLR; Järvi et al.,

95 2012; Kleingeld et al., 2018; Lietzke et al., 2015; Matthews and Schume, 2022; Nemitz et al., 2002; Park and Schade, 2016; Velasco et al., 2009) or power-correlation (Helfter et al., 2011) between traffic volumes and CO_2 fluxes.

Though the yearly averaged $EFs_{traffic}$ likely reduce complexities in modelling, this method is susceptible to the seasonal bias owing to variations in natural and anthropogenic CO_2 emissions such as changes in photosynthesis and respiration by urban vegetation, space heating, degree of incomplete combustion of vehicles, etc. as Helfter et al. (2011) described with

100 varying $EFs_{traffic}$ among seasons. Thus, more than a year of measurement is required to properly integrate the seasonal changes in EFs with careful consideration in analysis for skewness in the number of observations in each season. In some regions of the world, measured number of data imbalance among seasons are unavoidable due to the inherent natural variabilities especially vulnerable with open path sensors during rainy seasons.

As an alternative to this aspect, we suggest an analytical approach to extract CO_2 EFs among the differences in day of week

105 (DOW) pairs from EC flux observations not only to minimize the seasonal bias but also to enable EFs evaluations with relatively short-term period than many years of measurements. From this practice, we were able to see the subtlety in inferring the magnitude of urban vegetation uptakes as well as the importance in the seasonal bias free CO_2 EFs, in addition to the comparison with existing emission inventory.

2 Methods

110 ### 2.1 Site description

To directly assess the CO_2 EFs from various sources in an urban area, EC system was set up and operated at Gwangju in Korea (35° 10' 0.0048" N, 126° 54' 59.9904" E) from November 2017 to August 2018 (Figure 1) just before the start of the typhoon season. This city is a legitimate test bed for anthropogenic CO_2 EFs estimation, not only due to its high population density (2,920 people km^{-2}) with various land use types (commercial, residential and recreational area with industrial

115 facilities as well, information available from the website of the Environmental Geographic Information Service, EGIS, https://egis.me.go.kr/main.do) but also due to its flat terrain especially in the central area where the City Hall is located. In addition, this city setting is even more ideal for the aim of this study since the Gwangju Industrial Complex, which hosts an automobile production plant, is located 2 km away from the city hall in eastern direction (Figure 2a).

Atmospheric
Chemistry
and Physics
Discussions
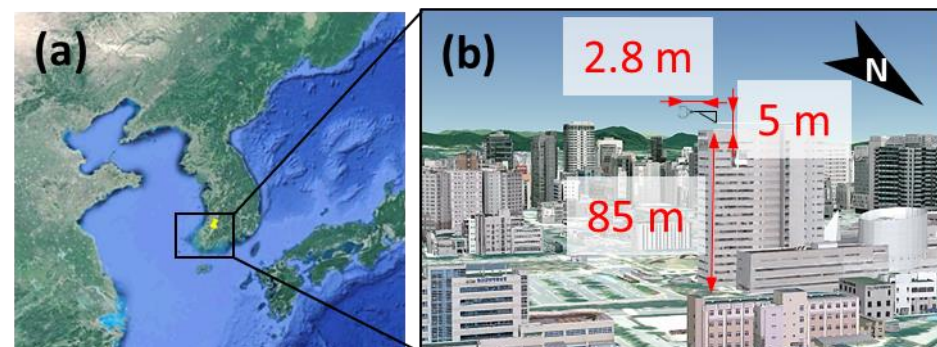
120 **Figure 1.** (a) Location of the study area in Gwangju, Korea, © Google Maps 2022 and (b) instrumental set-up position on top of the Gwangju city hall building visualized in 3-dimensional view provided by the geospatial information open platform, Vworld.

The CO_2 flux measuring system was installed on the helideck of the Gwangju city hall (90 m above the ground – building height: 85 m, helideck: 3 m and measuring system structure: 2 m, shown in Figure 1b) to fulfill the height requirements for

125 EC flux measurements. Roth et al. (2017) suggested that the flux measuring height should be at least 2 to 4 times higher than the canopy height. The mean canopy height(z_h, 12.33 m) of the study area is determined from the building height data available from the Electronic Architectural administration Information System (EAIS, https://cloud.eais.go.kr/). The required information for the footprint analysis were extracted as roughness length (z_0) of 1.6 m and displacement height (z_d) of 9.1 m from the inferred relation of roughness elements density and z_0/z_h and z_d/z_h by Grimmond and Oke (1999).

130 Our EC system was installed outside of inertial sublayer (average of 25 m within footprint area and 80 m near the city hall, following Grimmond and Oke, 1999) and sufficiently lower than the planetary boundary layer (Bottema, 1997) which varies from 0.3 km to 1.2 km at this site, determined from the balloon-borne measurements of potential temperature profiles acquired by Republic of Korea Air Force at Gwangju airport (4 times in a day, 3:00, 9:00, 15:00, and 21:00, local time, from 2001 to 2018).

135 To minimize the wind distortion caused by the city hall building, the EC flux measuring system was installed on the helideck and outreached by 2.8 m outside of the building in a diagonal direction as shown in Figure 1b. Further interpretations of flux measurements are limited to the direction where the wind distortions were minimized, based on Computational Fluid Dynamics (CFD) calculation (Figure S1).

2.2 Measurement method

140 We used a 3-D sonic anemometer (CSAT3B, Campbell Scientific Inc., Utah, USA) and an open path CO_2 and H_2O analyser (LI-7500RS, LI-COR, Nebraska, USA) operated at 10 Hz for the flux measurements. From the data sets, half hour fluxes of CO_2 and H_2O, as well as latent and sensible heat, were calculated based on EC method as shown in equation (1), using the SmartFlux 2 (LI-COR) software,

$$F = \overline{w'c_x'} \tag{1}$$

145   where F represents the vertical flux of individual scalar (x) which can be evaluated from the averages (shown as an upper

bar in equation 1) of the covariance (represented as ′ in equation 1) of vertical wind velocity (w) and the abundance of x

(c_x), under the assumptions that mean vertical wind speed is zero and the changes in air density is negligible.

As the first pre-processing step, raw data were de-spiked; acceptable ranges of c and w were defined as ±3σ and ±5σ from

the mean, following Vickers and Mahrt (1997). The outranged observed c_{co2} and w were treated as spikes, thus replaced

150   with mean for further analysis. Then, 2-D axis rotation was performed to make the average vertical wind speed become zero

($\overline{w} = 0$) with double rotation method as Kaimal and Finnigan (1994). Calculated fluxes were averaged every 30 min with the

use of 5 min block average to reflect the slow changes in CO_2 concentration. Then, Webb–Pearman–Leuning (WPL)

correction (Webb et al., 1980) was applied to compensate for the effect of air density fluctuation.

As a quality control (QC) scheme, steady state and turbulence characteristic tests were performed by following Mauder and

155   Foken (2004) to filter out the periods of drastic CO_2 concentration changes and too stagnant condition where EC assumption

breaks. Only the 30 min flux data points which fall in the interquartile range of 6 continuous 5 min fluxes were used, and this

results in 18.3% data reduction. Furthermore, friction velocity threshold (u_*>0.2) was applied only for accounting sufficient

turbulent condition, which results in 9.4% data rejection. Due to the intrinsic nature of open-path nondispersive infrared

(NDIR) sensor for high frequency CO_2 measurement, data influenced by precipitation and high relative humidity (>90%)

160   were removed (3.1%). Also, data points with sharp and/or large changes in rotation angles (more than 3° of rotation) were

filtered out (7.8%) to exclude measurements under agitating condition owing to external physical factors. With all the

filtering processes, 37% of data has been discarded.

2.3 Footprint analysis

To apportion the CO_2 sources in flux measurement, footprint analysis was conducted using two different approaches-

165   Kormann and Meixner (2001) and Kljun et al., (2004) models to process non-neutral condition and to evaluate broader

ranges of boundary layer stratifications. Here, footprint boundaries were defined to confine 70% of average total flux during

the measurement period. Detailed calculations and parameterizations are described in S2 of the Supporting Information.

Fetches were drawn with 5° bins, starting from north as 0° with increase in clockwise direction, centred at the city hall as

shown in Figure 2a. The atmospheric stability was also evaluated from the length scale (ζ) with Obukhov length (L)

170   calculation; unstable (stable) condition is determined as when $ζ = (z_m - z_d)/L$ is lower (higher) than -0.05 (0.2). Other

conditions are classified as near neutral condition. Site characteristics regarding atmospheric stability are described in S2.

To assess the quantitative contributions of the individual sources, the wind directions were split into two sectors; (1) the

Eastern Industrial Area (EIA, 45º-100º) and (2) the Southern Green Area (SGA, 100º-225º), based on whether or not the

fetch includes the automobile production plant and urban vegetation (Figure 2).

2.4 Emission factor estimation

2.4.1 Vehicular CO_2 emission

Flux of CO_2 (F_{CO2}) measurements over SGA were used to estimate $EF_{traffic}$ for minimizing the influence of industrial CO_2 emission by comparing inferred traffic counts and F_{CO2}. SLR and DOW difference methods were used for $EF_{traffic}$ to gauge the influence of seasonal changes in anthropogenic and biogenic CO_2 emissions. The distinct difference in DOW F_{CO2} provides adequate information for $EF_{traffic}$ with minimum seasonal biases, since the photosynthetic activities and space heating hardly change between weekend and weekdays within a week frame. Hence, the ratio of the flux and traffic count difference (ΔF and ΔT) between weekday and weekend were used as $EF_{traffic}$ (Eq. 2).

$$EF_{traffic\_DOW} = \frac{\Delta F}{\Delta T} = \frac{F_{weekday} - F_{weekend}}{T_{weekday} - T_{weekend}} \qquad (2)$$

Since no in situ traffic counts were available near the city hall, it was inferred from the measurements of inbound and outbound of 6 highway tolls surrounding Gwangju (Gwangju, Donggwangju, Hakun, Songam, Seogwangsan and Donggwangsan), together with the occasional observations on the adjacent crossroads on the eastern and southern side of the city hall (Gyesu and Sangmu district), in hourly resolution. The locations of tolls and crossroads are shown in Figure S3. The highway toll data are available from Korea Expressway Corporation's public data portal (http://data.ex.co.kr/) and occasional survey information are available upon request to Gwangju Metropolitan City Transportation Department (https://www.gwangju.go.kr/traffic/).

For 30 minute traffic counts, under the assumption of even distribution of traffic within an hour, averages of ratios between adjacent crossroads and highway tolls were used not only over the study period but also for the years of 2019 and 2020 (2017-2020 and 2019-2020 for weekdays and weekend) since weekend and Friday data were only available after 2019. Since weekday (weekend) traffic survey only happened from Tuesday to Thursday (Sunday), Monday and Friday (Saturday) ratios inferred from weekday averages (Sunday only) were not used for $EF_{traffic}$ but $EF_{industry}$. Detailed descriptions on diurnal traffic patterns with respect to days in a week are in supporting information S3. Briefly, distinct bimodal patterns which peaked in the morning and afternoon rush hours were observed (as also seen in Figure 5a) for the weekdays with slight difference in Monday and Friday (Figure S4). Meanwhile, weekend patterns showed delays in morning peaks with broader afternoon peaks (Figure 5a) and Sunday was used as weekend. To maximize the number of samples for DOW difference, two pairs of weekend-weekdays were made, one in the previous week and one after that which centered around a specific Sunday.

Time window of 7:00 to 10:00 was used as a default morning hours and ranges from 6:00 to 10:00 with varying averaging window size of 1 to 4 hours were applied as robustness tests in $EF_{traffic}$ estimations. The linear correlations between traffic counts and CO_2 fluxes were extracted considering uncertainties in both scalars defined as 1 standard deviation in binning window, and the errors in parameters were computed using Monte Carlo simulation assuming Gaussian distribution. For

convenience, $EFs_{traffic}$ obtained through the day of week difference are named as $EF_{traffic\_DOW}$, in order to distinguish with that from the SLR method ($EF_{traffic\_SLR}$).

One should note that the inferred traffic counts should be treated as an activity index which represents the relative amount of car fleet than the actual integrated number of cars within the fetch. Thus special treatments are required to compare the

210     $EFs_{traffic}$ with other studies, since the degree of closeness in traffic volume with respect to the total traffic counts in a footprint likely varies among studies.

2.4.2 Industry and heat related CO₂ emission

The data from EIA were used to evaluate the emission factor from industrial area ($EF_{industry}$). The CO_2 emissions from on-road vehicles, inferred from the previous section, were subtracted from the EC flux measurements to extract the industrial

215   emission. Even with the difference in contribution of other CO_2 emission/uptake sources than traffic and industry in EIA and SGA, DOW CO_2 fluxes difference owing to them is expected to be negligible, since their emissions/uptakes hardly change within a week. The traffic density difference between SGA and EIA was corrected based on the ratio of the traffic survey of two representative crossroads.

In reality, the CO_2 emission from the car manufacturing company only happens over the factory site (0.298 km²), therefore,

220   extracted $EF_{industry}$ was calculated by normalizing the areal coverage of the facility against the whole area in EIA (4.32 km²).

As a conservative estimation in $EF_{industry}$, the time window of 11:00 to 14:00 was chosen not only because the normal operation hours are 6:00 to 22:00 during weekdays but also because the traffic volume changes with respect to time are relatively low, and this minimizes error accumulation. As a sensitivity test, different time windows from 10:00 to 14:00 with

225   varying averaging ranges of 2 to 4 hours were used.

To gauge the amount of CO_2 emission related to space heating during the low temperature season, analysis via HDD estimation as by Kleingeld et al. (2018) was performed. Briefly, HDD was calculated by multiplying the heating temperature and the number of days when the temperature was below 18 ℃, assuming that the heating tendency stops once the temperature reached 18 ℃. For September and October in 2018, inferred HDD with second order regression were used

230   (purple line in Figure S5). Both EIA and SGA data were considered for $EFs_{heating}$ with time window of 10:00 to 14:00, when the CO_2 fluxes showed clear difference above and below 18 ℃ with light traffic condition. The $EF_{heating}$ was estimated from the slope of CO_2 fluxes and temperatures under the temperature limit and the sensitivity tests were conducted by varying the threshold from 10 to 22 ℃ with 2 ℃ bins.

2.4.3 Year round CO₂ emission and vegetation contribution

235   In this section, we describe how we scale up to evaluate the yearly emission of CO_2 among activities in city scale to compare it with Gwangju greenhouse gas emission inventory of 2018 (available from International Climate & Environment Center,

2018). This inventory provides the emissions of CO_2 by the lowest administrative district of urban, named as "Dong" in Korea; a total of 10 dongs were overlapped within the footprint. Since the district boarders mismatched with the footprint boundary, the normalized emissions by area were compared.

240   To calculate the annual CO_2 emission in city scale, areal coverage of individual activities was considered. Since the on-road vehicle emission happens all over the fetch due to the densely populated traffic pathways, half hour varying median traffic volume (4,023 cars) inferred from crossroad surveys was used with areal coverage of road (impervious, 5.32 km^2). For the total CO_2 emission from heat, $EFs_{heating}$ were considered within total area of residential, commercial and other buildings in the fetch (3.10 km^2) with HDD of 2,330 °C in a year.

3 Results and discussion

3.1 Footprint and land use type analysis

Analysed footprints by following Kormann and Meixner 2001 (in blue) and Kljun 2004 (in red) are shown in Figure 2a which stretched to roughly 3.5 km radius in radial direction. Large differences are observed in southwest to northeast region in clockwise direction (shaded with red and blue), which likely originated from wind distortion owing to the structure of the building and helideck. Meanwhile, the fetches from northeast to southwest side agree well; based on the CFD models, less than 20% of wind speed distortions were observed for the wind blowing from 45° to 225° (shown in Figure S1). Thus, for the rest of the analysis, the averaged footprint between two methods with wind sector within the range of 45°-225° was used.
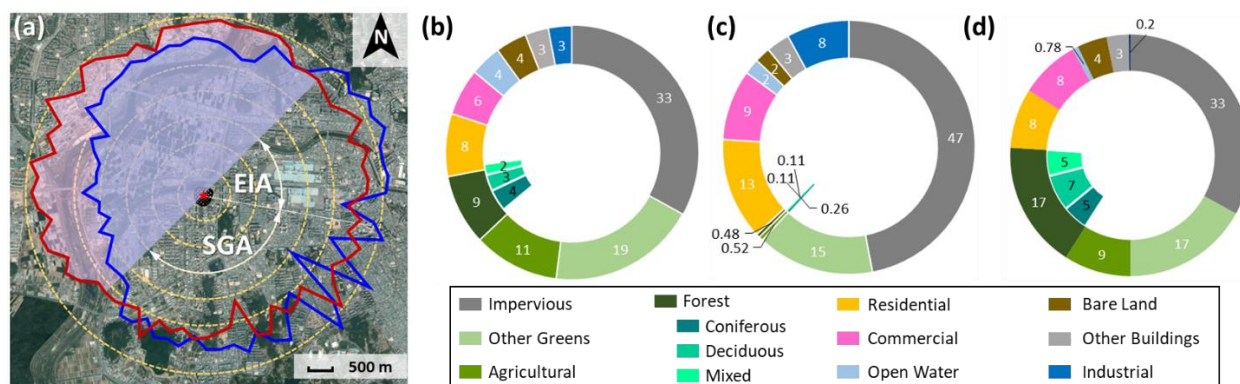

Figure 2. (a) Footprint analyses on the land use map (red and blue lines by Kljun (2004) and Korman and Meixner, (2001), respectively) with the fraction of land use types in percentage for (b) all radial direction, (c) EIA (Eastern Industrial Area) and (d) SGA (Southern Green Area) sector. The red and blue shaded regions in (a) were not used. Black patched area and red stars in the center area of (a) represent the invisible region owing to the sensor height and location of city hall. © Google Maps 2022

The land use type within the fetch is shown in Figure 2. The complex land use character in the central area of Gwangju within the footprint (Figure 2b) ranges from impervious road and parking lot (34.2%), greens (39% including forests, agricultural areas of rice paddy, farm field and orchards as well as other greens of yards and graves), residential (7.80%),

Atmospheric
Chemistry
and Physics
Discussions
Open Access
EGU

commercial (6.22%) to industrial (2.64%). Figure 2c and d further categorize land use components for EIA and SGA; the major differences are whether the area includes industrial area or not (EIA: 7.87% vs SGA: 0.21%) as well as the fraction of forest and agricultural area (EIA: 1% vs SGA: 26%) except the fraction of yards and graves marked as other greens.

265   **3.2 CO₂ measurement descriptions**
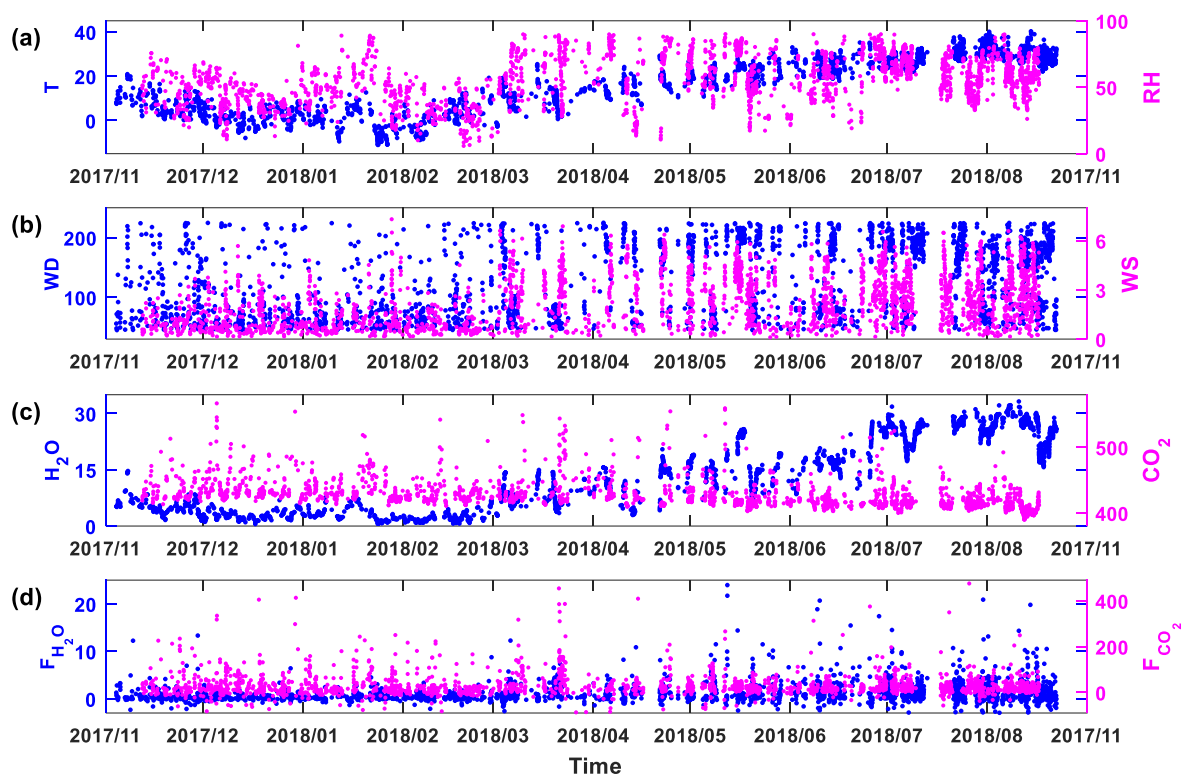
Figure 3. Time series of (a) temperature (T, °C) and relative humidity (RH, %), (b) wind direction (°) and speed (m s^{-1}), (c) mixing ratios of H_2O and CO_2 (ppth, part per thousand, and ppm, part per million), and (e) fluxes of H_2O and CO_2 (F_{H2O} and F_{CO2}, **mmol m^{-2} s^{-1}** and **µmol m^{-2} s^{-1}**, respectively).

270

Time series of wind sector filtered temperature (T), relative humidity (RH), wind direction (WD), wind speed (WS), mixing ratios and fluxes of H_2O and CO_2, (H_2O, CO_2, F_{H2O} and F_{CO2}, respectively) are shown in Figure 3. The averages (interquartile range) of T, RH and WS were 17.17(±10.57) °C, 56.32(±15.70) % and 2.36(±1.28) m s^{-1}, respectively. The observed mixing ratios of H_2O and CO_2 were 14.57(±7.45) ppth (part per thousand) and 425.58(±13.00) ppm (part per million) and their

275   fluxes were 1.12(±0.68) mmol m^{-2} s^{-1} and 28.26(±14.14) µmol m^{-2} s^{-1}, respectively.

T, RH and H_2O mixing ratio clearly showed seasonal changes in March and June from winter to spring and spring to summer. After July, monsoon starts as indicated by H_2O abundance and RH. Measured F_{H2O} showed larger variations after March than wintertime, likely due to active evaporation processes as temperature increases. As opposed to F_{H2O}, observed

F_{CO2} had more variation in cold than warm season, mainly due to the strong vertical concentration gradients reflecting the

280   active changes in CO_2 emission/uptake processes (i.e. space heating, respirations, etc.). The F_{CO2} with positive sign indicates that Gwangju is a net CO_2 source like other cities in the world as listed in Table 1, and comparable to Firenze and London (Matese et al., 2009; Ward et al., 2015). The observed F_{CO2} range agrees well with previously reported CO_2 emission estimation (yearly average of 26.6 ± 11.2 µmol m^{-2} s^{-1}) by expenditure pattern (Moran et al., 2018).

However, our direct measurements of F_{CO2} showed clear seasonal variabilities (Figure 3 and Figure S6). Monthly changes in

285   F_{CO2} showed distinct patterns in cold (November–February: 26.59 ± 18.13 µmol m^{-2} s^{-1}) and warm (April–August: 17.32 ± 11.26 µmol m^{-2} s^{-1}) seasons. Meanwhile, mixing ratio of CO_2 gradually decreased from January (441.28 ± 12.85 ppm) to August (421.03 ± 10.55 ppm) and recovered in winter period (November to December: 443.97 ± 14.88 ppm) even though it is hard to determine when it exactly happened due to the missing data in September and October 2018.
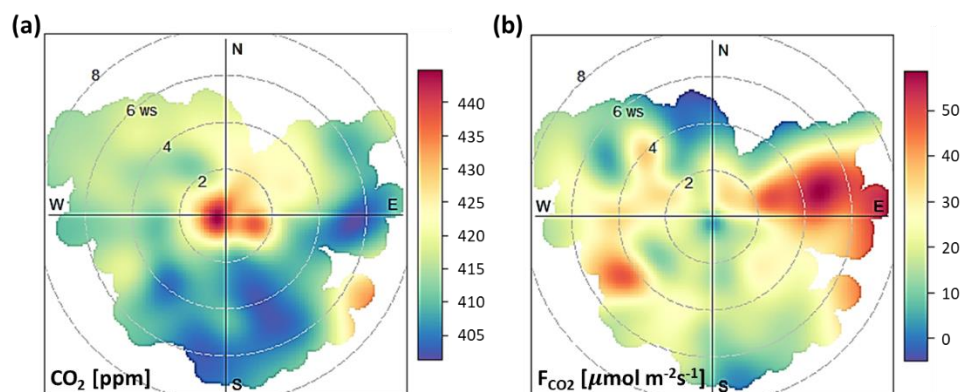
290   **Figure 4.** Polar plots of (a) CO_2 mixing ratio and (b) F_{CO2} centered at where the measurements were conducted.

The polar plots of CO_2 mixing ratio and flux are shown in Figure 4, where the color represents wind speed weighted CO_2 mixing ratio and F_{CO2}. Enhanced CO_2 mixing ratio was observed under low wind speed condition indicating strong influence of main city roads near the city hall where intensive activities take place. Meanwhile, the polar plot of F_{CO2} contrasted with

295   that of concentration. Strong F_{CO2} signals were observed when wind blew from East-northeast (ENE) to southeast mainly where the car manufacturing factory exists. On the other hand, the relatively low F_{CO2} signature was observed from South–southeast (SSE) to south area where the forests are situated. The averaged highest F_{CO2} was observed with wind speed around 4.7 m s^{-1} from ENE direction in EIA. We would like to clarify that the F_{CO2} data from Southwest (SW) to Northeast (NW) were not considered to be interpreted due to possible wind distortion by the city hall building.

(a)
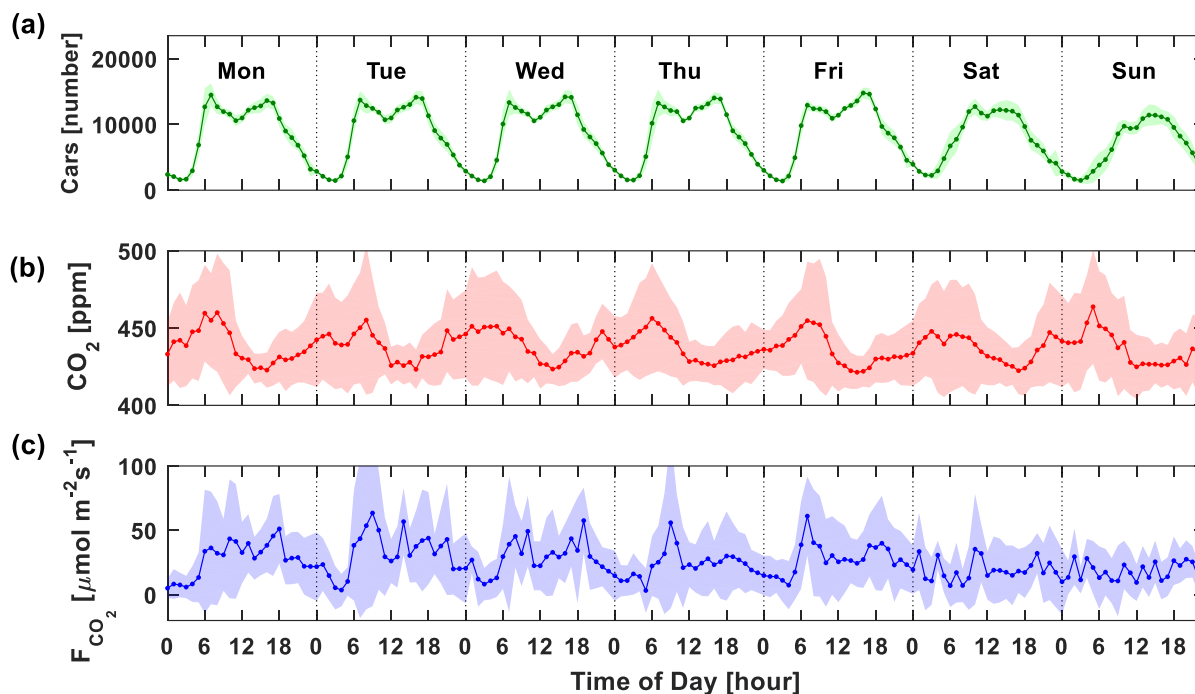
Figure 5. Weekly diurnal patterns of (a) traffic volumes, (b) CO_2 mixing ratio and (c) F_{CO2}. Dotted marker with lines and area represent mean and interquartile range of each factor.

The weekly diurnal patterns of CO_2 and F_{CO2} along with traffic counts are shown in Figure 5. CO_2 mixing ratio (Figure 5b) increased until 6:00-7:00 and then decreased until around 18:00 and recovered the next morning, regardless of day of the week, mainly due to changes in vertical mixing as PBL develops after the sun rises and variations in urban vegetation activity on top of daily anthropogenic emissions as explained by (Sargent et al., 2018). On the other hand, apparent F_{CO2} difference between weekday and weekend was observed (Figure 5c); weekday flux was higher than that of the weekend. It is mainly attributed to changes in human activities over a week such as traffic volume related with commuting fleet (shown in Figure 5a) and operations of the car manufacturing facilities. Apparent consistency in diurnal variations of F_{CO2} and traffic volume during weekday (Monday to Friday) was observed with two local maxima around 6:00-9:00 and 17:00-19:00 (Figure S7). Meanwhile, broader enhancement traffic counts with relatively weak or no apparent peaks in F_{CO2} patterns existed over Saturday and Sunday (also shown in Figure S7). From this relation, $EF_{traffic}$ was extracted as follows.

3.4 Emission factors (EFs) estimations

With varying wind sectors, observed F_{CO2} can be further analysed to apportion EFs of each of the sources under the assumption of well mixing up to the measurement height. One should note that even with the careful design of instrumental setup (i.e. located at constant flux layer on flat fetch) and filtration scheme for only considering active turbulent condition,

we cannot rule out the potential CO_2 loss by advection as well as accumulation near the surface which could not be detected by our sensor. With limited information in CO_2 gradient measurements, horizontal seepage and vertical storage corrections

320 were not performed. Thus, we only provide EFs of lower limit in emission than actual strengths.

3.4.1 $EF_{traffic}$ emission

$EF_{traffic}$, from the observations with windblown from SGA using SLR, was quantified as 0.0012($\pm$0.0011, 92% error) μmol m^{-2} s^{-1} car^{-1} (RMSE=3.01) as shown in Figure 6a, which falls in the range of other previous findings; this value is lower than Arnhem (0.075, Kleingeld et al., 2018), Basel (0.011, Lietzke et al., 2015), and Mexico City (1.53-3.87, Velasco et al., 2005)

325 but in similar range with Houston (0.002, Park and Schade,2016), Helsinki (0.006, Järvi et al., 2012), and Edinburgh (0.0017, Nemitz et al., 2002). However, as mentioned in Sect. 2.5.1, $EF_{traffic\_SLR}$ is inherently vulnerable to seasonal variations especially for the case when the measurement cannot represent whole year round seasonality. The intercept of fitted line (shown in Figure 6a) indicating CO_2 emission under 0 traffic condition was 4.79 μmol m^{-2} s^{-1} with large variability range of $\pm$12.53 μmol m^{-2} s^{-1} likely referring the various degree of CO_2 emission/uptake among seasons and the large

330 uncertainty in regression slope ($\pm$0.0011 μmol m^{-2} s^{-1} car^{-1}) has likely arisen due to this reason as well.

Meanwhile, $EF_{traffic\_DOW}$ was extracted as 0.017 ($\pm$0.011, 65% error) μmol m^{-2} s^{-1} car^{-1} (RMSE=3.66) which is more than an order of magnitude higher than $EF_{traffic\_SLR}$ (Figure 6b) but falls in those of Basel and Mexico City conditions. Even though our number agrees with other works, however, as mentioned in section 2.4.1, simple comparison with $EF_{traffic}$ previous works is not recommended, since the inferred traffic counts only describe the degree of busyness of on-road

335 vehicles in the fetch rather than the actual number of total cars; crossroad surveys are inherently lower than the total amount of traffic in fetch area. Thus the differences in $EFs_{traffic}$ among studies likely arise from the variations in degree of consistency in their traffic volume with total number of cars as well as actual difference in $EF_{traffic}$.

One should note that the intercept and its range of fitted line with DOW method drastically reduced to 2.09 $\pm$ 4.34 μmol m^{-2} s^{-1}, which is a sign of effective removal in seasonality. However, the cause of non-zero intercept of F_{CO2} indirectly indicates

340 the existence of CO_2 emission with weekend and weekday changes in SGA other than traffic. Unaccounted CO_2 emissions from industrial, commercial and other activities may explain it, and thus an interesting topic for future investigations. We do not believe that human respiration influences on it due to the implementation of DOW difference in F_{CO2}. The sensitivity tests of $EF_{traffic\_SLR}$ and $EF_{traffic_{DOW}}$ showed 13.9 and 27.06% (1 standard deviations) changes, respectively. The uncertainties in $EF_{traffic\_SLR}$ and $EF_{traffic\_DOW}$ were estimated as 92% and 65%, correspondingly from their linear

345 regression fitting uncertainties.
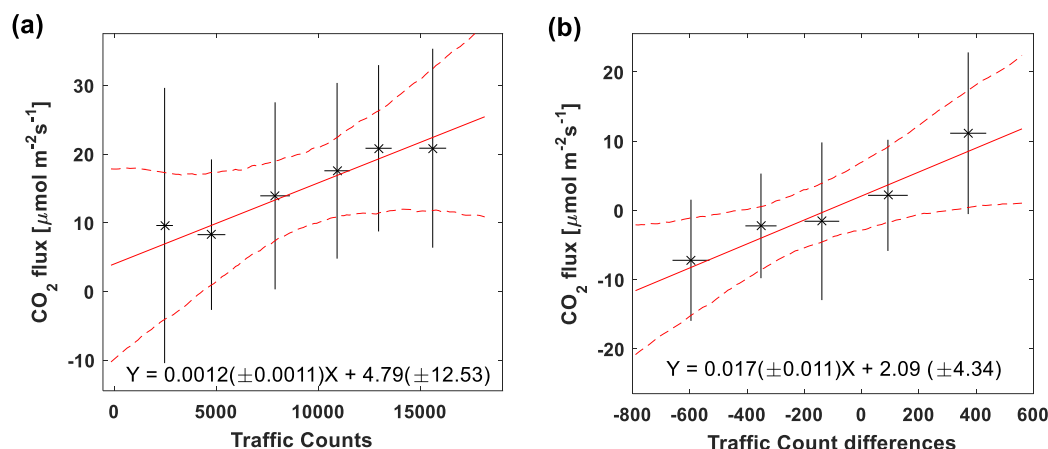
Figure 6. Estimation of traffic emission factor ($EF_{traffic}$) from the relation of F_{CO2} with respect to the number of cars, estimated by (a) simple linear regression (SLR) and (b) day of week difference (DOW).

3.4.2 $EF_{industry}$ and EF_{heat} estimation

Data from EIA were used for $EF_{industry}$ estimation where the measured F_{CO2} contains CO_2 emission features of residential, commercial, industrial, traffic as well as urban vegetation. As similar to $EF_{traffic\_DOW}$, by taking the day of week difference in F_{CO2}, we intended to ease out the contributions from residential and commercial area as well as vegetation under the assumption that their CO_2 emission/uptake patterns are held relatively constant in a week. Figure S8 shows the diurnal pattern differences in DOW for traffic and F_{CO2} in EIA. From the $EF_{traffic\_DOW}$ and traffic counts in eastern direction, the lower limit of $EF_{industry}$ was estimated as 103.25 (±42.18, 41% error) μmol m^{-2} s^{-1} normalized to the areal coverage (0.341 km^2) of car manufacturing company and varied by 54.25 % (1 standard deviation) as the result of sensitivity tests. Considering normal operation hours of 6:00-22:00, from Monday to Friday, yearly emission was assessed as 66 (±34) kt CO_2 km^{-2} under the assumption of constant emission over the operation hours except during holidays.

15
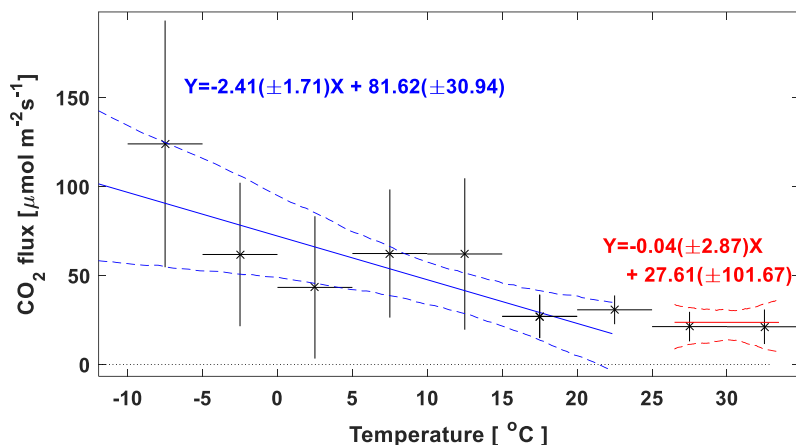
Figure 7. F_{CO2} changes with respect to the ambient temperature. Blue solid and dashed lines represent linear regression and confidence band, respectively, for cold period and red lines for warm period.

In regard to heat related CO_2 emission, calculated HDD of each month (shown in Figure S5) was used. From the relation between temperature and CO_2 flux shown in Figure 7, where CO_2 fluxes tended to decrease as the temperature increased up to 18 °C, the $EF_{heating}$ was estimated as 2.41(±1.71, 71% error) µmol m^{-2} s^{-1} °C^{-1} similar magnitude with those in Arnhem, Łódź and London (Kleingeled et al., 2018; Pawlak et al., 2011 and Ward et al., 2015) and thus year round emission of 21(±15.1) kt CO_2 km^{-2} was evaluated.

We presumed that the large range in $EF_{heating}$ estimations was mainly due to the larger variabilities in F_{CO2} in lower temperature, not only owing to the missing data in September and October especially when heating tendency started but also owing to relatively stratified condition, thus, larger vertical gradients in cold periods. Sensitivity test of $EF_{heating}$ was conducted by changing the threshold temperature, and 28.2% changes were drawn for $EF_{heating}$.

4 Conclusions

Direct CO_2 exchange quantified by EC method from urban center in Gwangju and estimated EFs with land use characters are summarized in Table 2. Even though F_{CO2} measurements for September and October were missing, year round emissions of individual activities were able to be estimated from seasonal bias free EFs extraction strategies; since the $EF_{traffic\_DOW}$ and $EF_{industry}$ were inferred from DOW and $EF_{heating}$ were extracted from the relation of F_{CO2} with temperature, no specific monthly dependency was expected.

Table 2. Summary of emission factors (***EF***) and annual emissions for individual activities, only for the parameters inferred from day of week difference due to the limitations in data coverage for September and October.

	Measured Flux	Traffic	Industry	Heat	Vegetation
EFs (error)	28.3 $\mu mol\ m^{-2}\ s^{-1}$ (23%)	0.017 $\mu mol\ m^{-2}\ s^{-1}\ car^{-1}$ (65%)	103.3 $\mu mol\ m^{-2}\ s^{-1}$ (42%)	2.41 $\mu mol\ m^{-2}\ s^{-1}$ $°C^{-1}$ (71%)	- (109%)
Area	14.1 km^2	5.23 km^2	0.33 km^2	3.1 km^2	4.63 km^2
Activity	-	4023 car	3,856 hr	2,330 °C	-
Yearly emission	554 kt CO_2 yr^{-1} 39 kt CO_2 km^{-2} yr^{-1} 10.7 kg C m^{-2} yr^{-1}	497 kt CO_2 yr^{-1} 95 kt CO_2 km^{-2} yr^{-1} 25.9 kg C m^{-2} yr^{-1}	21 kt CO_2 yr^{-1} 63 kt CO_2 km^{-2} yr^{-1} 17.21 kg C m^{-2} yr^{-1}	66 kt CO_2 yr^{-1} 21 kt CO_2 km^{-2} yr^{-1} 5.83 kg C m^{-2} yr^{-1}	-29 kt CO_2 yr^{-1} -6.28 kt CO_2 km^{-2} yr^{-1} -1.7 kg C m^{-2} yr^{-1}

385   The year round total CO_2 emissions for individual activities were estimated from the information of hourly median of traffic counts, operations hours for normal days within the industrial area and areal coverage of heat related land use (details are in Table S1), and quantified as 497, 21, and 66 kt CO_2 yr^{-1}, respectively, thus the major source of CO_2 in a year in Gwangju is on-road vehicle and heat generation (85 and 11 %, correspondingly).

From these quantities with observed flux of CO_2, the plants influence on CO_2 exchange including photosynthesis and respiration can be estimated as the net balance of total emissions among all activities with observation; -29 (-27) kt CO_2 yr^{-1}

390   (only considering industry emission in EIA region), which is 5 % in total exchange in a year, was evaluated from $EF_{traffic\_DOW}$. Under the consideration of vegetation coverage in the fetch (4.63 km^2) as net CO_2 uptake area, the total carbon intake by vegetation was evaluated as 1.7 (1.6) kg C m^{-2} yr^{-1} which falls in the range of previous researches (0.28-2.45 kg C m^{-2} yr^{-1}, (Febriani et al., 2018; Jo, 2002; Leu, 1990; Liu and Li, 2012; Rowntree and Nowak, 1991).

 One should note that even though our evaluated CO_2 uptake strength agrees with literature, the uncertainty ranges are large

395   (109%), since it was quantified from the subtle balance among individual emissions with large variabilities. In addition, we did not account for the CO_2 emission from human respiration, thus we only provide lower limit of plant roles than actual.

Interestingly, with $EF_{traffic\_SLR}$, additional 432 kt CO_2 yr^{-1} of CO_2 emission source(s) is(are) required to reconcile the observed F_{CO2} which is unlikely the case for Gwangju. We conclude that this is a direct evidence in the importance of integrating all seasonal features in *EFs* estimation; missing data of specific month likely induced incorrect estimation due to

400   the failure in assimilating all seasonal features (fall characteristics in our case), thus seasonal bias free method i.e. $EF_{traffic\_DOW}$ is a more proper strategy in annual CO_2 emission estimation.
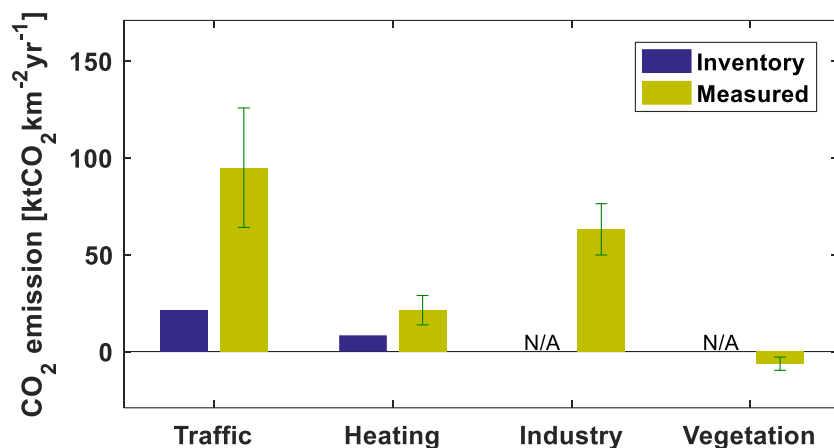
Figure 8. Comparison of CO_2 emissions between this study (dark yellow) and Gwangju emission inventory in 2017(dark blue). The whiskers represent uncertainties evaluated by Monte-Carlo bootstrap sensitivity test. Industrial emission and plant uptake are not available (N/A) from the inventory.

Based on our *EFs* estimations, both the annual CO_2 emissions of traffic and space heating (95 and 21 kt CO_2 km^{-2} yr^{-1}) were more than 2.5 times higher than those of the emission inventory for Gwangju in 2017 (21.4 and 8.37 kt CO_2 km^{-2} yr^{-1}, respectively; Figure 8). We presume that even with the systematic traffic counts with energy and fuel consumption monitoring, either the existence of fugitive CO_2 emissions or imperfection in *EF*s parameterization can be the reason for the underestimation. Thus, more efforts on the existing emission inventory validations are required. Unfortunately, we were not able to compare the annual CO_2 emission/uptake owing to the car manufacturing facility in EIA and urban vegetation, since the inventory was not compiled for it. Thus, site-specific emission inventories for individual facilities and validations are also needed in near future. In addition, more researches to understand the limited role of urban vegetation in CO_2 sequestrations are required as well as efforts to make this fact be known to the general public.

Even though we only provide lower limit estimations, our research results urge the necessity of emission inventory validation for establishing strategies that are more realistic to mitigate climate change. In this aspect, EC flux technique with careful analysis method is a useful tool even with relatively short-term period of measurements.

Data availability

All raw data can be provided by the corresponding author upon request.

Atmospheric
Chemistry
and Physics
Discussions

Authors contributions

KEM took charge of the whole project starting from initiation to data analysis and wrote the manuscript with contributions from all co-authors. JM deployed the instrument and processed the data and BP and SL facilitated the instrument maintenance and edited the paper. KHK contributed on CFD modelling work.

425 **Competing interests**

The authors declare that they have no competing interests.

Acknowledgements

References

430 Baldocchi, D., Falge, E., Gu, L., Olson, R., Hollinger, D., Running, S., Anthoni, P., Bernhofer, C., Davis, K., Evans, R., Fuentes, J., Goldstein, A., Katul, G., Law, B., Lee, X., Malhi, Y., Meyers, T., Munger, W., Oechel, W., Paw, U. K. T., Pilegaard, K., Schmid, H. P., Valentini, R., Verma, S., Vesala, T., Wilson, K. and Wofsy, S.: FLUXNET: A New Tool to Study the Temporal and Spatial Variability of Ecosystem-Scale Carbon Dioxide, Water Vapor, and Energy Flux Densities, Bull. Am. Meteorol. Soc., 82(11), 2415–2434, doi:10.1175/1520-0477(2001)082<2415:FANTTS>2.3.CO;2, 2001.

435 Bergeron, O. and Strachan, I. B.: CO2 sources and sinks in urban and suburban areas of a northern mid-latitude city, Atmos. Environ., 45(8), 1564–1573, doi:10.1016/j.atmosenv.2010.12.043, 2011.

Björkegren, A. and Grimmond, C. S. B.: Net carbon dioxide emissions from central London, Urban Clim., 23, 131–158, doi:10.1016/j.uclim.2016.10.002, 2018.

Bottema, M.: Urban roughness modelling in relation to pollutant dispersion, Atmos. Environ., 31(18), 3059–3075, 440 doi:https://doi.org/10.1016/S1352-2310(97)00117-9, 1997.

Burri, S., Frey, C., Parlow, E. and Vogt, R.: Co 2 Fluxes and Concentrations Over an Urban Surface in Cairo / Egypt, seventh Int. Conf. Urban Clim., (July), 27–30, 2009.

Christen, A., Coops, N. C., Crawford, B. R., Kellett, R., Liss, K. N., Olchovski, I., Tooke, T. R., Van Der Laan, M. and Voogt, J. A.: Validation of modeled carbon-dioxide emissions from an urban neighborhood with direct eddy-covariance 445 measurements, Atmos. Environ., 45(33), 6057–6069, doi:10.1016/j.atmosenv.2011.07.040, 2011.

Conte, M., Donateo, A. and Contini, D.: Characterisation of particle size distributions and corresponding size-segregated turbulent fluxes simultaneously with CO2 exchange in an urban area, Sci. Total Environ., 622–623, 1067–1078, doi:10.1016/j.scitotenv.2017.12.040, 2018.

Coutts, A. M., Beringer, J. and Tapper, N. J.: Characteristics influencing the variability of urban CO2 fluxes in Melbourne,
450   Australia, Atmos. Environ., 41(1), 51–62, doi:10.1016/j.atmosenv.2006.08.030, 2007.

Crawford, B. and Christen, A.: Spatial source attribution of measured urban eddy covariance CO2 fluxes, Theor. Appl.
Climatol., 119(3–4), 733–755, doi:10.1007/s00704-014-1124-0, 2015.

Crawford, B., Grimmond, C. S. B. and Christen, A.: Five years of carbon dioxide fluxes measurements in a highly vegetated
suburban area, Atmos. Environ., 45(4), 896–905, doi:10.1016/j.atmosenv.2010.11.017, 2011.

455   Desjardins, R. L.: A technique to measure CO2 exchange under field conditions, Int. J. Biometeorol., 18(1), 76–83,
doi:10.1007/BF01450667, 1974.

Doll, C. N. H., Muller, J. P. and Morley, J. G.: Mapping regional economic activity from night-time light satellite imagery,
Ecol. Econ., 57(1), 75–92, doi:10.1016/j.ecolecon.2005.03.007, 2006.

Druckman, A. and Jackson, T.: The carbon footprint of UK households 1990-2004: A socio-economically disaggregated,
460   quasi-multi-regional input-output model, Ecol. Econ., 68(7), 2066–2077, doi:10.1016/j.ecolecon.2009.01.013, 2009.

Febriani, A. P., Soeprobowati, T. R. and Maryono, M.: Analysis of Urban Forest Needs as Anthropogenic (CO2) Gas
Absorbent in Semarang City, E3S Web Conf., 31, 1–5, doi:10.1051/e3sconf/20183107007, 2018.

Gately, C. K., Hutyra, L. R., Wing, I. S. and Brondfield, M. N.: A bottom up approach to on-road CO2 emissions estimates:
Improved spatial accuracy and applications for regional planning, Environ. Sci. Technol., 47(5), 2423–2430,
465   doi:10.1021/es304238v, 2013.

Ghosh, T., Elvidge, C. D., Sutton, P. C., Baugh, K. E., Ziskin, D. and Tuttle, B. T.: Creating a global grid of distributed
fossil fuel CO2 emissions from nighttime satellite imagery, Energies, 3(12), 1895–1913, doi:10.3390/en3121895, 2010.

Goret, M., Masson, V., Schoetter, R. and Moine, M. P.: Inclusion of CO2 flux modelling in an urban canopy layer model and
an evaluation over an old European city centre, Atmos. Environ. X, 3(September 2018), 100042,
470   doi:10.1016/j.aeaoa.2019.100042, 2019.

Grimmond, C. S. B. and Oke, T. R.: Aerodynamic properties of urban areas derived from analysis of surface form, J. Appl.
Meteorol., 38(9), 1262–1292, doi:10.1175/1520-0450(1999)038<1262:APOUAD>2.0.CO;2, 1999.

Grimmond, C. S. B., King, T. S., Cropley, F. D., Nowak, D. J. and Souch, C.: Local-scale fluxes of carbon dioxide in urban
environments: Methodological challenges and results from Chicago, Environ. Pollut., 116(SUPPL. 1), doi:10.1016/S0269-
475   7491(01)00256-1, 2002.

Helfter, C., Famulari, D., Phillips, G. J., Barlow, J. F., Wood, C. R., Grimmond, C. S. B. and Nemitz, E.: Controls of carbon
dioxide concentrations and fluxes above central London, Atmos. Chem. Phys., 11(5), 1913–1928, doi:10.5194/acp-11-1913-
2011, 2011.

Hirano, T., Sugawara, H., Murayama, S. and Kondo, H.: Diurnal variation of CO2 flux in an urban area of Tokyo, Sci.
480   Online Lett. Atmos., 11(July), 100–103, doi:10.2151/sola.2015-024, 2015.

International Climate & Environment Center: 2018 Greenhouse Gas Inventory Report in Gwangju Metropolitan City,
Gwangju, Korea., 2018.

Isaksen, E. T. and Narbel, P. A.: A carbon footprint proportional to expenditure - A case for Norway?, Ecol. Econ., 131, 152–165, doi:10.1016/j.ecolecon.2016.08.027, 2017.

485 Järvi, L., Nordbo, A., Junninen, H., Riikonen, A., Moilanen, J., Nikinmaa, E. and Vesala, T.: Seasonal and annual variation of carbon dioxide surface fluxes in Helsinki, Finland, in 2006-2010, Atmos. Chem. Phys., 12(18), 8475–8489, doi:10.5194/acp-12-8475-2012, 2012.

Jo, H. K.: Impacts of urban greenspace on offsetting carbon emissions for middle Korea, J. Environ. Manage., 64(2), 115–126, doi:10.1006/jema.2001.0491, 2002.

490 Kaimal, J. C. and Finnigan, J. J.: Atmospheric Boundary Layer Flows: Their Structure and Measurement, Oxford University Press, New York., 1994.

Katul, G., Lai, C. T., Schäfer, K., Vidakovic, B., Albertson, J., Ellsworth, D. and Oren, R.: Multiscale analysis of vegetation surface fluxes: From seconds to years, Adv. Water Resour., 24(9–10), 1119–1132, doi:10.1016/S0309-1708(01)00029-X, 2001.

495 Kennedy, C., Steinberger, J., Gasson, B., Hansen, Y., Hillman, T., Havránek, M., Pataki, D., Phdungsilp, A., Ramaswami, A. and Mendez, G. V.: Greenhouse gas emissions from global cities, Environ. Sci. Technol., 43(19), 7297–7302, doi:10.1021/es900213p, 2009.

Kennedy, C., Steinberger, J., Gasson, B., Hansen, Y., Hillman, T., Havranek, M., Pataki, D., Phdungsilp, A., Ramaswami, A. and Mendez, G. V.: Methodology for inventorying greenhouse gas emissions from global cities, Energy Policy, 38(9), 4828–

500 4837, doi:10.1016/j.enpol.2009.08.050, 2010.

Kerkhof, A. C., Benders, R. M. J. and Moll, H. C.: Determinants of variation in household CO2 emissions between and within countries, Energy Policy, 37(4), 1509–1517, doi:10.1016/j.enpol.2008.12.013, 2009.

Kleingeld, E., van Hove, B., Elbers, J. and Jacobs, C.: Carbon dioxide fluxes in the city centre of Arnhem, A middle-sized Dutch city, Urban Clim., 24(June), 994–1010, doi:10.1016/j.uclim.2017.12.003, 2018.

505 Kljun, N., Calanca, P., Rotach, M. W. and Schmid, H. P.: A simple parameterisation for flux footprint predictions, Boundary-Layer Meteorol., 112(3), 503–523, doi:10.1023/B:BOUN.0000030653.71031.96, 2004.

Kordowski, K. and Kuttler, W.: Carbon dioxide fluxes over an urban park area, Atmos. Environ., 44(23), 2722–2730, doi:10.1016/j.atmosenv.2010.04.039, 2010.

Kormann, R. and Meixner, F. X.: An analytical footprint model for non-neutral stratification, Boundary-Layer Meteorol.,

510 99(2), 207–224, doi:10.1023/A:1018991015119, 2001.

Lee, S., Lee, S.-W., Jeon, G.-Y. and Hong, W.-H.: A study on distribution characteristics of the transportation carbon dioxide emission using the prediction of traffic volume – A case of the Daegu, J. Archit. Inst. Korea Plan. Des., 29(6), 21–28, 2013.

Leip, A., Skiba, U., Vermeulen, A. and Thompson, R. L.: A complete rethink is needed on how greenhouse gas emissions

515 are quantified for national reporting, Atmos. Environ., 174(December 2017), 237–240, doi:10.1016/j.atmosenv.2017.12.006, 2018.

Leu, S.: Forests and Carbon Dioxide, Swiss Rev. World Aff. No. 2, 10–13, 1990.

Liang, S. and Wang, J., Eds.: Estimate of vegetation production of terrestrial ecosystem, in Advanced Remote Sensing (Second Edition), pp. 581–620, Academic Press., 2020.

520 Lietzke, B., Vogt, R., Feigenwinter, C. and Parlow, E.: On the controlling factors for the variability of carbon dioxide flux in a heterogeneous urban environment, Int. J. Climatol., 35(13), 3921–3941, doi:10.1002/joc.4255, 2015.

Liu, C. and Li, X.: Carbon storage and sequestration by urban forests in Shenyang, China, Urban For. Urban Green., 11(2), 121–128, doi:10.1016/j.ufug.2011.03.002, 2012.

Liu, H. Z., Feng, J. W., Järvi, L. and Vesala, T.: Four-year (2006-2009) eddy covariance measurements of CO 2 flux over an 525 urban area in Beijing, Atmos. Chem. Phys., 12(17), 7881–7892, doi:10.5194/acp-12-7881-2012, 2012.

Lu, H. and Liu, G.: Spatial effects of carbon dioxide emissions from residential energy consumption: A county-level study using enhanced nocturnal lighting, Appl. Energy, 131, 297–306, doi:10.1016/j.apenergy.2014.06.036, 2014.

Matese, A., Gioli, B., Vaccari, F. P., Zaldei, A. and Miglietta, F.: Carbon dioxide emissions of the city center of Firenze, Italy: Measurement, evaluation, and source partitioning, J. Appl. Meteorol. Climatol., 48(9), 1940–1947, 530 doi:10.1175/2009JAMC1945.1, 2009.

Matthews, B. and Schume, H.: Tall tower eddy covariance measurements of CO2 fluxes in Vienna, Austria, Atmos. Environ., 274(November 2021), 118941, doi:10.1016/j.atmosenv.2022.118941, 2022.

Mauder, M. and Foken, T.: Documentation and Instruction Manual of the Eddy-Covariance Software Package TK3, Arbeitsergebnisse, (46), 60, ISSN 1614-8916 [online] Available from: http://nbn-535 resolving.de/urn/resolver.pl?urn:nbn:de:bvb:703-opus-8665%5Cnhttp://opus4.kobv.de/opus4-ubbayreuth/frontdoor/index/index/docId/681, 2004.

Menzer, O. and McFadden, J. P.: Statistical partitioning of a three-year time series of direct urban net CO2 flux measurements into biogenic and anthropogenic components, Atmos. Environ., 170, 319–333, doi:10.1016/j.atmosenv.2017.09.049, 2017.

540 Moran, D., Kanemoto, K., Jiborn, M., Wood, R., Többen, J. and Seto, K. C.: Carbon footprints of 13 000 cities, Environ. Res. Lett., 13(6), doi:10.1088/1748-9326/aac72a, 2018.

Moriwaki, R. and Kanda, M.: Seasonal and diurnal fluxes of radiation, heat water vapor, and carbon dioxide over a suburban area, J. Appl. Meteorol., 43(11), 1700–1710, doi:10.1175/JAM2153.1, 2004.

Nemitz, E., Hargreaves, K. J., McDonald, A. G., Dorsey, J. R. and Fowler, D.: Micrometeorological measurements of the 545 urban heat budget and CO2 emissions on a city scale, Environ. Sci. Technol., 36(14), 3139–3146, doi:10.1021/es010277e, 2002.

NOAA: The NOAA Annual Greenhouse Gas Index (AGGI), [online] Available from: https://www.esrl.noaa.gov/gmd/aggi/aggi.html (Accessed 8 July 2019), 2018.

Park, C. and Schade, G. W.: Anthropogenic and Biogenic Features of Long-Term Measured CO 2 Flux in North Downtown 550 Houston, Texas , J. Environ. Qual., 45(1), 253–265, doi:10.2134/jeq2015.02.0115, 2016.

Pawlak, W., Fortuniak, K. and Siedlecki, M.: Carbon dioxide flux in the centre of Łódź, Poland-analysis of a 2-year eddy covariance measurement data set, Int. J. Climatol., 31(2), 232–243, doi:10.1002/joc.2247, 2011.

Rana, G., Martinelli, N., Famulari, D., Pezzati, F., Muschitiello, C. and Ferrara, R. M.: Representativeness of carbon dioxide fluxes measured by eddy covariance over a mediterranean urban district with equipment setup restrictions, Atmosphere (Basel)., 12(2), doi:10.3390/atmos12020197, 2021.

Roth, M., Jansson, C. and Velasco, E.: Multi-year energy balance and carbon dioxide fluxes over a residential neighbourhood in a tropical city, Int. J. Climatol., 37(5), 2679–2698, doi:10.1002/joc.4873, 2017.

Rowntree, R. A. and Nowak, D. J.: Quantifying the role of urban forests in removing atmospheric carbon dioxide, J. Arboric., 17(10), 269–275, 1991.

Sabbatini, S., Mammarella, I., Arriga, N., Fratini, G., Graf, A., Hörtnagl, L., Ibrom, A., Longdoz, B., Mauder, M., Merbold, L., Metzger, S., Montagnani, L., Pitacco, A., Rebmann, C., Sedlák, P., Šigut, L., Vitale, D. and Papale, D.: Eddy covariance raw data processing for CO 2 and energy fluxes calculation at ICOS ecosystem stations, Int. Agrophysics, 32(4), 495–515, doi:10.1515/intag-2017-0043, 2018.

Sargent, M., Barrera, Y., Nehrkorn, T., Hutyra, L. R., Gately, C. K., Jones, T., Mckain, K., Sweeney, C., Hegarty, J., Hardiman, B., Wang, J. A. and Wofsy, S. C.: Correction: Anthropogenic and biogenic CO2 fluxes in the Boston urban region (Proceedings of the National Academy of Sciences of the United States of America (2018) 115 (7491-7496) DOI: 10.1073/pnas.1803715115), Proc. Natl. Acad. Sci. U. S. A., 115(40), E9507, doi:10.1073/pnas.1815348115, 2018.

Satterthwaite, D.: Cities' contribution to global warming: Notes on the allocation of greenhouse gas emissions, Environ. Urban., 20(2), 539–549, doi:10.1177/0956247808096127, 2008.

Schmid, H. P.: Source areas for scalars and scalar fluxes, Boundary-Layer Meteorol., 67(3), 293–318, doi:10.1007/BF00713146, 1994.

Schmidt, A., Wrzesinsky, T. and Klemm, O.: Gap filling and quality assessment of CO2 and water vapour fluxes above an urban area with radial basis function neural networks, Boundary-Layer Meteorol., 126(3), 389–413, doi:10.1007/s10546-007-9249-7, 2008.

Shi, K., Chen, Y., Yu, B., Xu, T., Chen, Z., Liu, R., Li, L. and Wu, J.: Modeling spatiotemporal CO2 (carbon dioxide) emission dynamics in China from DMSP-OLS nighttime stable light data using panel data analysis, Appl. Energy, 168, 523–533, doi:10.1016/j.apenergy.2015.11.055, 2016.

Shusterman, A. A., Kim, J., Lieschke, K. J., Newman, C., Wooldridge, P. J. and Cohen, R. C.: Observing local CO2 sources using low-cost, near-surface urban monitors, Atmos. Chem. Phys., 18(18), 13773–13785, doi:10.5194/acp-18-13773-2018, 2018.

Stagakis, S., Chrysoulakis, N., Spyridakis, N., Feigenwinter, C. and Vogt, R.: Eddy Covariance measurements and source partitioning of CO2 emissions in an urban environment: Application for Heraklion, Greece, Atmos. Environ., 201(August 2018), 278–292, doi:10.1016/j.atmosenv.2019.01.009, 2019.

Turner, A. J., Shusterman, A. A., McDonald, B. C., Teige, V., Harley, R. A. and Cohen, R. C.: Network design for

585   quantifying urban CO2 emissions: Assessing trade-offs between precision and network density, Atmos. Chem. Phys., 16(21), 13465–13475, doi:10.5194/acp-16-13465-2016, 2016.

Turner, A. J., Kim, J., Fitzmaurice, H., Newman, C., Worthington, K., Chan, K., Wooldridge, P. J., Köehler, P., Frankenberg, C. and Cohen, R. C.: Observed Impacts of COVID-19 on Urban CO2 Emissions, Geophys. Res. Lett., 47(22), 1–6, doi:10.1029/2020GL090037, 2020.

590   Ueyama, M. and Ando, T.: Diurnal, weekly, seasonal, and spatial variabilities in carbon dioxide flux in different urban landscapes in Sakai, Japan, Atmos. Chem. Phys., 16(22), 14727–14740, doi:10.5194/acp-16-14727-2016, 2016.

Velasco, E. and Roth, M.: Cities as net sources of CO2: Review of atmospheric CO2 exchange in urban environments measured by eddy covariance technique, Geogr. Compass, 4(9), 1238–1259, doi:10.1111/j.1749-8198.2010.00384.x, 2010.

Velasco, E., Pressley, S., Allwine, E., Westberg, H. and Lamb, B.: Measurements of CO2 fluxes from the Mexico City urban

595   landscape, Atmos. Environ., 39(38), 7433–7446, doi:10.1016/j.atmosenv.2005.08.038, 2005.

Velasco, E., Pressley, S., Grivicke, R., Allwine, E., Coons, T., Foster, W., Jobson, B. T., Westberg, H., Ramos, R., Hernández, F., Molina, L. T. and Lamb, B.: Eddy covariance flux measurements of pollutant gases in urban Mexico City, Atmos. Chem. Phys., 9(19), 7325–7342, doi:10.5194/acp-9-7325-2009, 2009.

Vesala, T., Järvi, L., Launiainen, S., Sogachev, A., Rannik, Ü., Mammarella, I., Siivola, E., Keronen, P., Rinne, J., Riikonen,

600   A. and Nikinmaa, E.: Surface-atmosphere interactions over complex urban terrain in Helsinki, Finland, Tellus, Ser. B Chem. Phys. Meteorol., 60 B(2), 188–199, doi:10.1111/j.1600-0889.2007.00312.x, 2008.

Vickers, D. and Mahrt, L.: graphDBSummary, J. Atmos. Ocean. Technol., 14, 512–526, 1997.

Ward, H. C., Kotthaus, S., Grimmond, C. S. B., Bjorkegren, A., Wilkinson, M., Morrison, W. T. J., Evans, J. G., Morison, J. I. L. and Iamarino, M.: Effects of urban density on carbon dioxide exchanges: Observations of dense urban, suburban and

605   woodland areas of southern England, Environ. Pollut., 198, 186–200, doi:10.1016/j.envpol.2014.12.031, 2015.

Webb, E. K., Pearman, G. I. and Leuning, R.: Correction of flux measurements for density effects due to heat and water vapour transfer, Q. J. R. Meteorol. Soc., 106(447), 85–100, doi:10.1002/qj.49710644707, 1980.

Wofsy, S. C., Goulden, M. L., Munger, J. W., Fan, S. M., Bakwin, P. S., Daube, B. C., Bassow, S. L. and Bazzaz, F. A.: Net exchange of CO2 in a mid-latitude forest, Science (80-.)., 260(5112), 1314–1317, doi:10.1126/science.260.5112.1314,

610   1993.

Zhang, X., Lee, X., Griffis, T. J., Baker, J. M. and Xiao, W.: Estimating regional greenhouse gas fluxes: An uncertainty analysis of planetary boundary layer techniques and bottom-up inventories, Atmos. Chem. Phys., 14(19), 10705–10719, doi:10.5194/acp-14-10705-2014, 2014.

Zhang, X., Wu, J., Peng, J. and Cao, Q.: The uncertainty of nighttime light data in estimating carbon dioxide emissions in

615   China: A comparison between DMSP-OLS and NPP-VIIRS, Remote Sens., 9(8), 1–20, doi:10.3390/rs9080797, 2017.